INSTITUT DE FRANCE
Académie des sciences

Comptes Rendus
Physique

Nicolas Bonod and Yuri Kivshar

All-dielectric Mie-resonant metaphotonics

Volume 21, issue 4-5 (2020), p. 425-442

Published online: 19 November 2020
Issue date: 16 December 2020

https://doi.org/10.5802/crphys.31

Part of Special Issue: Metamaterials 1
Guest editors: Boris Gralak (CNRS, Institut Fresnel, Marseille, France) and Sébastien Guenneau (UMI2004 Abraham de Moivre, CNRS-Imperial College, London, UK)

Les Comptes Rendus. Physique *sont membres du Centre Mersenne pour l'édition scientifique ouverte*
www.centre-mersenne.org
e-ISSN : 1878-1535

Comptes Rendus
Physique
2020, 21, nº 4-5, p. 425-442
https://doi.org/10.5802/crphys.31

Metamaterials 1 / *Métamatériaux 1*

All-dielectric Mie-resonant metaphotonics

Méta-photonique diélectrique avec des résonateurs de Mie

Nicolas Bonod[*, a] **and Yuri Kivshar**[b, c]

[a] Aix Marseille Univ, CNRS, Centrale Marseille, Institut Fresnel, 13013 Marseille, France

[b] Nonlinear Physics Center, Research School of Physics, Australian National University, Canberra ACT 2601, Australia

[c] ITMO University, St. Petersburg 197101, Russia

E-mails: nicolas.bonod@fresnel.fr (N. Bonod), yuri.kivshar@anu.edu.au (Y. Kivshar)

Abstract. All-dielectric subwavelength structures made of high-refractive-index materials combine a unique set of advantages in comparison with their plasmonic counterparts. In particular, they can interact resonantly with light through the excitation of both electric and magnetic multipolar Mie-type resonances. This review discusses novel approaches to manipulate light with Mie-resonant dielectric subwavelength structures, spanning from individual nanoparticles to metasurfaces, and covering a broad range of effects, from near-field energy enhancement to far-field beam shaping.

Résumé. Les matériaux diélectriques à indice de réfraction élevé peuvent interagir de manière résonnante avec la lumière grâce à l'excitation de modes de Mie électriques et magnétiques. Cette revue présente un état de l'art du contrôle de la lumière par les résonances électriques et magnétiques de Mie dans les nanostructures diélectriques. Elle décrit tout d'abord la reproduction des conditions de Kerker pour un contrôle de la diffusion avant ou arrière de la lumière. Elle décrit ensuite l'intérêt des résonances de Mie pour (i) le contrôle de l'interaction entre la lumière et la matière dans les antennes optiques diélectriques (exaltation de champ proche, densité d'états et directivité d'émission), (ii) la génération d'états photoniques liés dans le continuum ou encore (iii) la génération de couleurs structurelles par des métasurfaces diélectriques.

Keywords. All-dielectric nanophotonics, Mie resonances, Kerker effect, Bound states in the continuum, Metaphotonics, Metasurfaces.

Mots-clés. Nanophotonique diélectrique, Résonances de Mie, Conditions de Kerker, Etats liés dans le continuum, Métaphotonique, Métasurfaces.

* Corresponding author.

1. Introduction

All-dielectric metamaterials were proposed in the 2000's to achieve an artificial optical magnetism without metals [1, 2]. They were based on materials with high values of dielectric permittivity, typically larger than 100. Composite materials with such high dielectric permittivities were proven to yield negative permeabilities when applying an effective medium theory [2]. Unfortunately, common materials studied in the visible and near infrared (near-IR) spectra feature much smaller values of dielectric permittivity, typically smaller than 20. This constraint limited the soar of all-dielectric metamaterials in the visible and near-IR spectra.

However, it was highlighted also in the 2010's that silicon (Si) nanoparticles feature low-order electric and magnetic Mie resonances [3–8] which can also be employed for the realization of optical magnetism, although Si exhibits much smaller dielectric permittivities (typically around 12). Soon after, in 2012 the first experimental observations with dark-field spectroscopy of a strong magnetic response of individual Si particles were reported by two experimental groups [9, 10]. The spectral response observed with dark-field spectroscopy in the visible and near-IR spectra evidenced several peaks associated with low-order electric and magnetic Mie resonances. In particular, the possibility to excite both electric or magnetic resonances, and to balance the weight between the electric and magnetic dipolar modes to tailor the scattering properties of the particles triggered a huge interest. The resonant interaction of electromagnetic waves with high-index nanostructures offers the possibility to engineer and control their phase and amplitude [11]. The possibility to combine electric and magnetic resonances inside the same dielectric nanostructure opened novel routes to develop planar metasurfaces able to tailor the phase of light as well as its transmittance and reflectance spectra.

Soon after, the field of "all-dielectric metamaterials", based on effective averaged parameters, has been replaced naturally by "metaphotonics" (or "meta-optics", also called "Mie-tronics") where not averaged parameters but individual resonances become important. This field is inspired by the physics of the magnetic dipole resonances and optical magnetism originating from the resonant dielectric nanostructures with high refractive index [12]. The concepts of meta-optics and all-dielectric resonant nanophotonics are driven by the idea to employ subwavelength dielectric Mie-resonant nanoparticles as "meta-atoms" for creating highly efficient optical metadevices, and the term "meta" is attributed to the importance of an optically-induced magnetic response.

Because of the unique optical resonances and their various combinations employed for realizing interference effects and strong localization of the electromagnetic fields, high-index nanoscale structures are expected to complement or even replace different plasmonic components in a range of potential applications. Moreover, many concepts developed for plasmonic structures, but fell short of their potential due to strong losses of metals at optical frequencies, can now be realized with Mie-resonant dielectric structures.

2. Mie resonances

Light scattering by small particles is a fundamental problem in optics and electromagnetism. It can be studied by solving Maxwell's equations in the spherical coordinates. This theory, called multipolar theory or Mie theory, was developed originally by Gustav Mie in 1908 [13] and improved by several contributors all over the XXth century [14, 15].

Spherical microstructures host high-order multipolar resonances associated with extremely high quality factors (Q factors) that are called whispering gallery modes. They are observed in almost lossless dielectrics such as silica or silicon nitride microstructured in microspheres or microdisks [16, 17]. When decreasing the size of the dielectric cavities from the micro to the sub-micrometer scale, the strength of the resonance weakens with refractive index typically

considered in whispering gallery modes (typically around $n \approx 1.3$ and $n \approx 1.9$). The order of the excited mode decreases with the size. The smallest size of an optical resonator is achieved when the lowest mode is excited. However, an efficient excitation of a low-order mode requires an increase of the refractive index, typically from 1.5 to values larger than 2.2 and ideally larger than 3. In the visible and near-IR spectra, semi-conductors such as silicon or germanium exhibit refractive index ranging between 3 and 4 while some oxides also feature nice optical properties such as titania.

Efficient resonant light-matter interactions at the nanoscale can be achieved for low-order resonances in sub-micrometer sized particles. Compared with high order multipolar whispering gallery modes, low-order resonances are characterized by smaller Q factors and a wider spectral response (see Figures 1(a–d)). The scattering cross section of a single dielectric particle is plotted in Figure 1(a), where R is the radius of a spherical particle. Several peaks can be observed over the visible spectrum. A multipolar decomposition of the scattered field (see Figure 1(b)) allows to identify the nature of the mode associated with each peak. When decreasing the wavelength, *i.e.* for the largest ratio between the wavelength and size of the scatterer, the first peak corresponds to the excitation of the magnetic dipolar mode, the second peak to the electric dipolar mode. The Mie resonances can also be obtained in non-spherical scatterers. This property results from the fact that the interest is brought in low-order resonances. Such resonances are less sensitive to high spatial frequencies than high-order multipolar resonances. That is the reason why a large set of geometries has been investigated to tailor low-order Mie resonances.

Spherical silicon particles can be fabricated with the laser ablation technique [19]. This technique is very convenient since it allows to disperse particles on glass cover-slips and to perform dark-field optical spectroscopy, see Figure 1(c). It is enlightening to observe such well defined electric and magnetic resonances that nicely match the numerical calculations. If the first interest of Mie resonances was brought in their far field response to retrieve for example the so-called Kerker conditions, one of the main interest of such resonances is to yield strong field intensities inside high-refractive-index materials.

It turns out that the terminology of "Mie resonance" is classically employed for describing resonances in dielectric particles. However, we stress that plasmonic and dielectric resonances can both be described by the Mie theory. In a sake of illustration, let us consider a silver particle at the frequency that maximizes its dipolar plasmonic resonances, *i.e.* at the frequency that maximizes its dipolar electric Mie coefficient a_1. It turns out that a dielectric scatterer can also maximize this Mie coefficient. An analytic expression between the two dielectric permittivities, of positive and negative real parts, derived in Ref. [18], permits to calculate the dielectric permittivity that maximizes the electric dipolar resonance, or in other words, the plasmonic resonance. The calculation of the scattering cross-section of the metallic and dielectric particles displayed in Figure 1(d) shows that the two particles can exhibit the same optical response. However, the magnetic response is almost negligible with spherical metallic particles and strong magnetic responses can be obtained only with more complex geometries.

The field of plasmonic metamaterials has investigated different geometries to overcome this limitation and to yield a strong magnetic response. Among a wide variety of plasmonic shapes, one can cite the U- and the Ω-shaped scatterers [20, 21]. Coupling a set of plasmonic scatterers that exhibit a resonant electric polarizability is also an efficient way to yield artificial magnetism [22]. The terminology employed to describe this effect is inspired by molecular chemistry where electronic orbitals of different atoms can couple. The coupling modifies the energy of the electronic orbitals and leads to the formation of bonding and anti-bonding chemical bonds [23]. The set of plasmonic scatterers is therefore called "plasmonic oligomers". This field of research aims at engineering the coupling between the different modes of the plasmonic scatterers to optimize either the electric or magnetic response of the plasmonic oligomers.

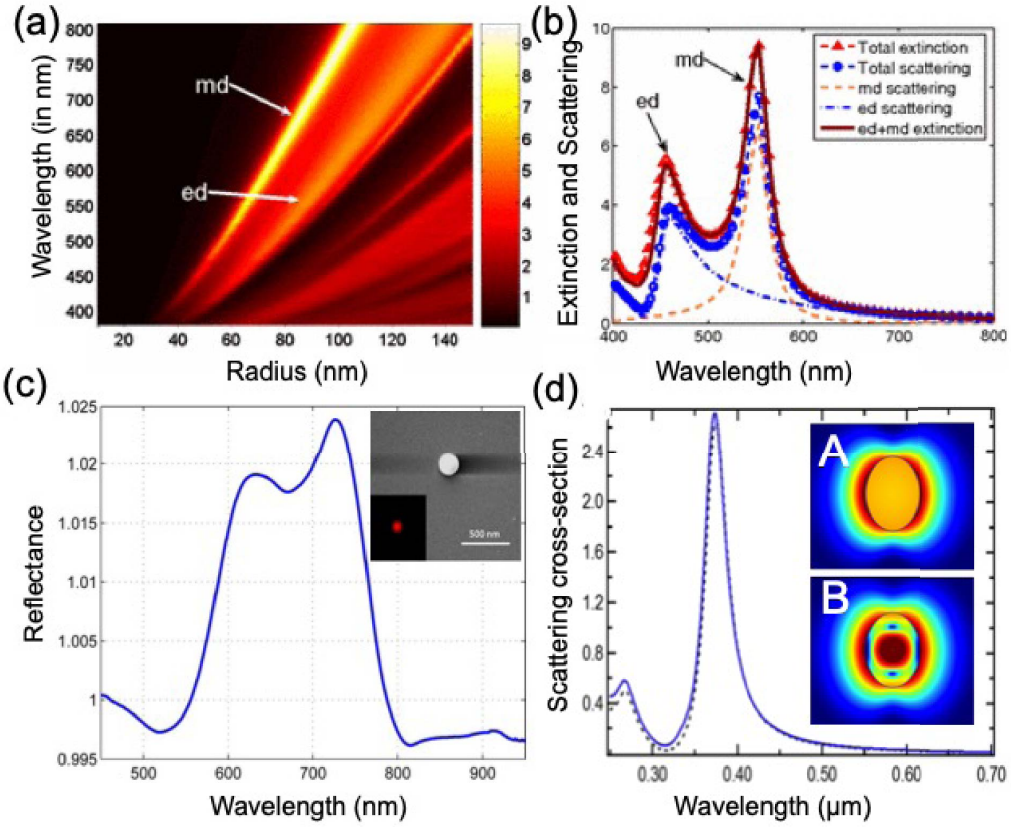

Figure 1. Scattering properties of subwavelength particles. (a) Scattering efficiency spectra of a spherical Si particle with the radius R in air. (b) Extinction and scattering spectra of a Si particle with $R = 65$ nm. The arrows indicate the electric dipole (ed) and magnetic dipole (md) contributions to the total efficiencies. Adapted with permission from [3]. (c) Experimental reflectance spectra of a 208 nm Si sphere on a glass substrate. Inset: Scanning Electron Microscopy (SEM) image of the corresponding Si nanoparticle and dark-field microscopic images. Adapted with permission from [10]. (d) Equivalence of Mie resonances in plasmonic and dielectric particles. Scattering cross-section with respect to the wavelength. Dotted line: silver particle A with $\epsilon = -2.5 + 0.5i$; Solid blue line: dielectric particle B with $\epsilon = 112 + 0.5i$. Both particles have the same diameter: 50 nm. Adapted with permission from [18].

The ability of spherical dielectric particles to yield a strong magnetic response is one of the main feature of Mie resonances. This property is at the core of many investigations with dielectric nanostructures to tailor the light scattering through the coherent excitation of electric and magnetic modes and also to enhance the magnetic interaction between matter and electromagnetic waves, *i.e.* the wave-matter interaction *via* the magnetic component of the field. The magnetic mode yields a strong magnetic response in the near field of the dielectric scatterer. The magnetic field distribution can be engineered and strong magnetic field intensities can be obtained. The strong magnetic response can also be used to engineer the magnetic local density of states and to promote magnetic spontaneous emission of quantum emitters. In the far field, the coherent excitation of both electric and magnetic dipoles leads to unique scattering properties.

3. Kerker effect and Kerker conditions

In 1983, Milton Kerker and co-authors [24] discovered an interesting effect in the scattering of electromagnetic waves by a spherical particle made of a magnetic material characterized by magnetic permeability μ and dielectric permittivity ϵ. This study revealed very unusual effect, nowadays called *Kerker effect*. More specifically, Kerker and his collaborators revealed the possibility to redirect the scattered radiation to either forward or backward direction, depending on the frequency. They discovered two conditions, known as *the first and second Kerker conditions*. The first Kerker condition corresponds to a cancellation of the backward scattering (with a maximum in the forward scattering), while the second Kerker condition corresponds to a deep minimum in the forward scattering direction. The backward and forward scattering are defined by the scattering along the axis of the incoming waves. The optical theorem states that the extinction cross-section of a scatterer can be cast with respect to its forward scattering, which means that the forward scattering cannot be canceled. Kerker and co-workers established that the first condition is obtained when $\epsilon = \mu$, and the second condition is satisfied when

$$\epsilon = -\frac{\mu - 4}{\mu + 1}.$$

Initially, this important study did not find a wide audience due to a lack of required magnetic materials, and also because the Kerker conditions require special values of the parameters.

Nevertheless, as was shown independently by two groups in 2011, the Kerker conditions can be extended to nonmagnetic dielectric spheres supporting both electric and magnetic Mie resonances [6, 25, 26]. This property of Mie scatterers to satisfy both Kerker conditions due to the electric and magnetic Mie resonances was actually one of the first unusual property investigated in this new field of all-dielectric metaphotonics. The artificial magnetism provided by the Mie resonances allows to mimic the anomalous scattering properties of magnetic spheres.

The Kerker conditions are predicted through the calculation of the electric and magnetic polarisabilities of the dielectric scatterer, α_e and α_h, respectively. It is convenient to derive the electric and magnetic polarisabilities from the elements of the $T_n^{(e,h)}$ matrix (e and h standing for electric and magnetic respectively), conventionally noticed a_n and b_n, with n standing for the multipolar orders:

$$\alpha_e = -T_n^{(e)} = \frac{3\mathrm{i}\epsilon a_1}{2k^3}, \quad \alpha_h = -T_n^{(h)} \frac{3\mathrm{i}b_1}{2\mu k^3}.$$

For a dipolar scatterer, *i.e.* a scatterer for which the multipolar Mie scattering coefficients a_n and b_n can be safely neglected for $n \geq 2$, the first Kerker condition is obtained when $a_1 = b_1$ while the second Kerker condition satisfies the relations: $\Re(\epsilon^{-1}\alpha_e) = -\Re(\mu\alpha_m)$ and $\Im(\epsilon^{-1}\alpha_e) = \Im(\mu\alpha_m)$ [25, 26]. These analytical derivations can be assessed by calculating and the scattering patterns of a single sphere at the first and second Kerker conditions [29] and first observed experimentally for microwaves [25, 30]. Experimental values of the scattered intensity of a sphere can be matched well with the theoretical results, as shown in Figures 2(a,b). Experimental observations of the Kerker conditions in the visible spectrum has been reported for Si and GaAs nanoparticles [27,31]. In Ref. [27], an AlGaAs particle was fabricated by reactive ion etching followed by a transfer on a transparent fused silica substrate. Bright field spectroscopy on a single particle allowed the measurement of the reflected spectrum and the observation of a cancellation of the reflected intensity in a short spectral range [27].

The first Kerker condition finds straightforward applications in the design of Huygens sources in planar metasurfaces [32]. This condition meets several conditions that make dipolar Mie scatterers ideal candidates to build metasurfaces: besides their weak losses, they can scatter light in the forward direction, with a maximum of forward light scattering when $a_1 = b_1$ while the phase of the polarisability of a dipolar scatterer experiences a phase shift of π at a resonance.

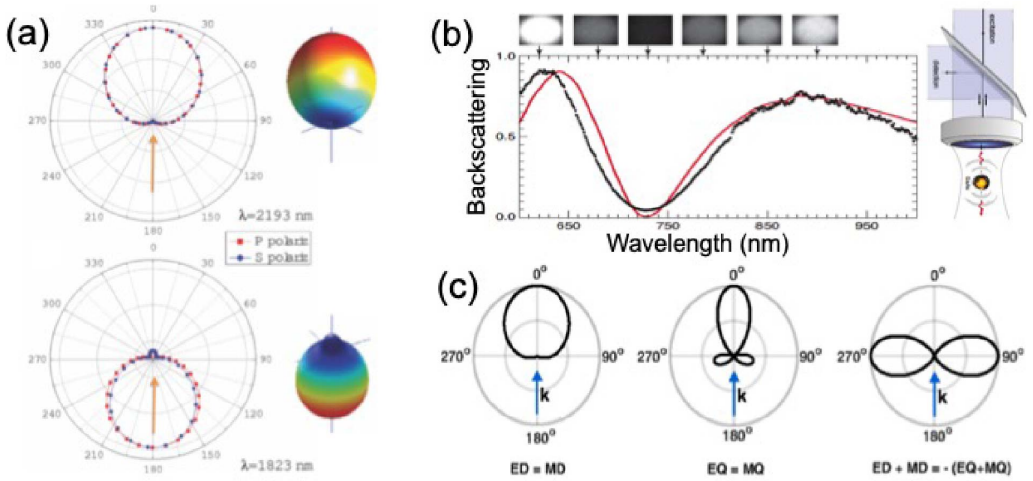

Figure 2. Kerker effects in dielectric nanoantennas. (a) Evidence of the Kerker effect in a germanium sphere. Scattering diagram plotted for the two polarization cases (TE (blue) and TM (red)) when illuminating a 140 nm Ge sphere at the wavelengths $\lambda = 2193$ nm (top; forward scattering) and $\lambda = 1823$ nm (bottom; backward scattering). Adapted with permission from [25]. (b) Observation of the Kerker effect in optics. Left: Spectrum of light intensity backscattered by an individual GaAs nanodisk of radius 90 nm. Black dotted curve: measurement; red curve: numerical spectrum. Right: sketch of the measurement: white light is weakly focused on a GaAs particle. Backscattered light is separated by a 50/50 beam-splitter and sent to a spectrometer. Adapted with permission from [27]. (c) Concept of the transverse Kerker effect. Electric dipole (ED) is in phase with a magnetic dipole (MD), and an electric quadrupole (EQ) is in phase with a magnetic quadrupole (MQ), whereas the dipoles are out of phase with the quadrupoles. Adapted with permission from [28].

When combining electric and magnetic resonances, the phase of the polarisability of a single Mie resonator can be tuned over 2π [32]. The forward light scattering being based on the excitation of both electric and magnetic dipolar resonances, this forward scattering can be associated with a strong modulation of the light phase. Efforts have been put to optimize the geometry of the scatterer to optimize the forward light scattering [33]. Regarding the second Kerker condition, we mention that besides the modulation of phase, it finds applications to develop highly refractive metasurfaces [34].

The extension of the Kerker effect to other multipoles has been discussed in a number of papers, and these studies have been summarized recently [35]. Here, we also mention a recently demonstrated novel effect of the so-called transverse scattering of light by Mie-resonant subwavelength particles with simultaneous suppression of both forward and backward scattering [28]. This generalized Kerker effect occurs when in-phase electric and magnetic dipoles become out of phase with the corresponding pairs of quadrupoles. Shamkhi *et al.* [28] obtained the general conditions for the simultaneous suppression of scattering in both forward and backward directions, and generalized these conditions to non-spherical particles, see Figure 2(c). They verified the concept in a proof-of-principle microwave experiment, with good agreement with analytical and numerical results, and also studied metasurfaces composed of the nanoparticles with the transverse scattering patterns. In a sharp contrast to Huygens' metasurfaces, these novel metasurfaces scatter neither forward nor backward, being almost invisible [36].

Subwavelength structures demonstrate many unusual optical properties which can be em-

ployed for a control of scattering of light and invisibility cloaking. Suppression of light scattering can be achieved for a uniform dielectric object with high refractive index, based on the novel physics of cascades of Fano resonances observed in the Mie scattering from a homogeneous dielectric rod [37]. Scattering cancellation and optical cloaking have been reported for a variety of systems based on dielectric metamaterials [38–40].

4. All-dielectric nanoantennas

Optical antennas are nanostructures aimed at manipulating spontaneous emission of solid-state emitters at room temperature [41]. Plasmonic antennas were proposed early in the 2000's, first to engineer the local density of states in the vicinity of metallic nanostructures [42–46], and second to control the direction of emission of quantum emitters [47]. This field of research has led to impressive results since metallic nanostructures can yield giant decay rates and can efficiently shape the emission pattern. Among the wide range of metallic antennas, Yagi–Uda antennas and corrugated antennas exhibit high gains in directivity [48, 49]. Self-assembled metallic particles were also proved to yield extremely high decay rates, either with DNA template nanoantennas in which is grafted a single fluorescent molecule [50, 51], or with gap plasmons obtained by depositing colloidal particles on metallic substrates and by inserting quantum emitters inside the extremely small nanogap separating a metallic film from a colloidal particle [52, 53].

Electromagnetic Mie resonances experienced in dielectrics with weak losses are very promising to develop highly radiative and directive optical antennas. The use of dielectric particles was first investigated with silica microspheres that host high multipolar orders [54]. The use of higher refractive index combined with a decrease of the size of dielectric particles was investigated numerically with a titania particle [55]. The titania particle was used to shape the emission pattern of an electric dipole located in the nanogap of a silver dimer of nanoparticles. The dimer was used to enhance the decay rates while the high refractive index was used to shape the emission direction into a narrow lobe [55]. A hybrid metal-dielectric antenna was experimentally developed in 2018 [56]. It was composed of a bow-tie gold nanoantenna coupled with 3 silicon nanorods. This antenna was fed by the photoluminescence of gold.

Silicon particles were numerically investigated in 2011 and 2012 to tailor the emission pattern of electric dipolar emitters. By studying the emission pattern of an electric dipole coupled with a silicon particle hosting electric and magnetic dipolar modes, it was showed as early as 2011 that the direction of emission can be optimized either in the backward or the forward direction [6]. The main interest of Mie resonant antennas comes from the possibility to couple the quantum emitter with both electric and magnetic modes [6–8]. The coherent excitation of electric and magnetic modes offers a higher degree of freedom to engineer the emission in a given direction through the phase and amplitude of electric and magnetic modes. The coherent excitation of electric and magnetic dipoles can be seen as an extension of the Kerker conditions in the near field, *i.e.* when the Mie resonator is excited from the near field. The emission of a quantum emitter coupled with a dielectric Mie resonator can therefore be maximized in either the forward or the backward directions. The gains in directivity that are obtained in these two conditions are higher than those that could be achieved with an antenna hosting a single mode resonance, *i.e.* an electric dipole resonance like in the case of spherical plasmonic nanoparticles.

Besides their strong interest to shape the emission pattern of solid-state emitters, dielectric Mie resonators are also very interesting to enhance the excitation strength of quantum emitters, to tailor their local density of states and to control their spontaneous emission rates. When compared with their plasmonic counterparts, the total decay rate enhancements yielded by dielectric antennas are smaller but the ratio between radiative and total decay rates can be larger thanks to smaller intrinsic losses. However, dielectric Mie resonators offer key properties

to manipulate spontaneous emission: (i) they can tailor decay rates of both electric and magnetic dipolar transitions, (ii) they exhibit weak intrinsic losses and can efficiently collect the emitted photons, (iii) semi-conductor based antennas can be easily integrated into photonic chips, (iv) internal fields can be engineered to boost the photoluminescence properties of emitters located inside the high refractive index material [57].

Controlling the electric or magnetic nature of the dipolar transition with Mie resonances, and more generally controlling higher order transition moments, is an inspiring way of investigation [58]. This field of research rapidly raised the interest since it coincided with the raise of interest in the higher order transition moments in rare earth ions [59–61]. Electric and magnetic resonances of Mie resonators were therefore investigated to promote either an electric or a magnetic transition of coupled rare-earth ions [62, 63]. However, from an experimental point of view, coupling rare earth ions with Mie resonators and more precisely locating the emitter at the position where the magnetic local density of states (LDOS) is maximum is very challenging. The main achievements in the control of magnetic spontaneous emission were reported only recently with either individual Si-based antennas [64] or Si-based metasurfaces [65].

If interest in Mie resonant antennas was initially driven by the original concept of magnetic spontaneous emission, they also offer a strong interest to enhance the electric LDOS that is suitable to enhance fluorescence of quantum dots or molecules (see Figure 3). Taking inspiration from plasmonic nanogap antennas [50, 51, 69, 70], dielectric dimer antennas were proposed to manipulate the spontaneous emission, as evidenced first numerically [62, 71] and in a second step experimentally [67, 68, 72]. The main challenge is to optimize the field outside the high refractive index and to yield strong electric field intensities with a strong contrast with the background in order to detect fluorescence signal of molecules located in the nanogap (see Figure 3). This method allows the enhancement of the electric field excitation on fluorescent molecules and to increase by several orders of magnitude their fluorescence signal [68, 72].

If dielectric gap antennas are based on the strong enhancement of the electric field intensity in the gap separating the two particles, a major interest of Mie resonant antennas lies in the fact that they can be fed directly inside the cavity where the Purcell factor is maximum [73]. The first result was reported in 2017 with quantum dots embedded in silicon nanodisks [74]. Let us notice that the concept of hybridization also applies to this case so that dimers and trimers of doped Si-nanodisks can be coupled to further boost the photoluminescence of quantum dots. The strong enhancement of the internal field intensity driven by Mie resonances can also be exploited to enhance the Raman signal of silicon particles [75, 76] and non linear signals. The richness of this field of research will undoubtedly lead to several outcomes in the upcoming years.

A very promising way of development is to consider active materials to design the photonic cavities (see Figure 4). For example, the high refractive index of diamond can be used to form a Mie resonant cavity around color centers [77, 78]. The resonant scattering of light on nanodiamonds due to the excitation of electric and magnetic dipolar modes has been evidenced (see Figure 4(a)). The photoluminescence of color centers can therefore benefit from Mie resonances. An enhancement of the photoluminescence of Nitrogen Vacancy (NV) color centers in nanodiamonds was reported recently: the fluorescence efficiency can be enhanced thanks to Mie resonances and the emission lifetime can be decreased [79] (see Figure 4(b)).

A very promising approach for developing active Mie resonators is to consider halide perovskites, a class of semi-conductor materials characterized by a high refractive index. The discovery of the exceptional excitonic properties almost 10 years ago triggered a huge interest to improve the efficiency of photovoltaics and light emitting devices [80]. Halide perovskites feature exceptional excitonic properties. Bridging the gap between this novel class of light emitting materials and Mie resonant cavities will lead to outcomes in integrated light sources [81]. Enhancement of the photoluminescence of halide perovskites was first reported in 2018 by considering par-

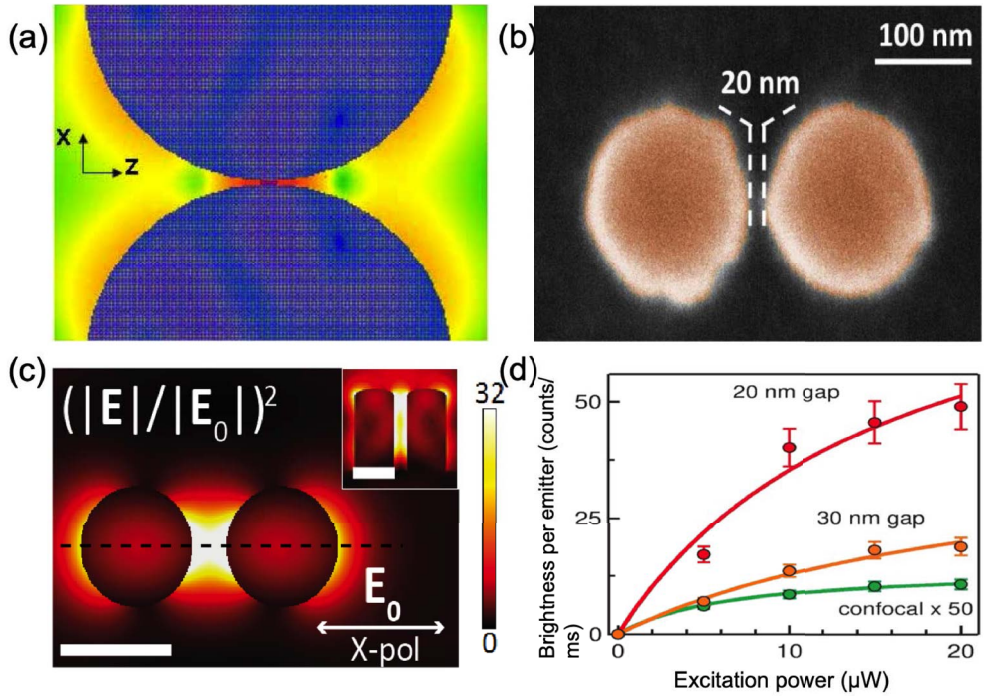

Figure 3. All-dielectric nanogap antennas. (a) Electric field distribution in the vicinity of a 20 nm nanogap separating two Si microdisks (diameter 2 μm, thickness of 200 nm) illuminated in normal incidence with an incident electric field linearly polarized along the x-axis at a wavelength of 2.437 μm. Adapted with permission from [66]. (b) SEM image of a silicon nanogap antenna fabricated with e-beam lithography. Diameter of 170 nm diameter, thickness of 60 nm and nanogap of 20 nm. (c) Enhancement of the electric field intensity yielded by a GaP dimer antenna composed of two GaP pillars, 100 nm in diameters, 200 nm in height and separated by a 35 nm nanogap. The field distribution is taken at mid-height (100 nm). Adapted with permission from [67]. (d) Brightness *per* emitter with respect to the emission power for two different nanogap lenghts, 20 nm and 30 nm, with the Si dimer nanogap antenna displayed in (b). Comparison with the brightness *per* emitter measured without antenna (measured signal × 50). Adapted with permission from [68].

ticles made of $MAPbI_3$ created by using a laser ablation technique on a perovskite thin film. A maximum of the photoluminescence signal was reported at the wavelength corresponding to the quadrupolar magnetic resonance [82]. The next challenge after performing Mie enhanced photoluminescence lies in the stimulated emission and the development of a novel class of laser cavities by forming Mie cavities in halide perovskites. The latest results were obtained with nanocubes made of $CsPbBr_3$ (see Figures 4(c–e)). High quality monocrystalline $CsPbBr_3$ nanocubes are first synthesized chemically on a sapphire substrate (see Figure 4(c)). Dark field spectrum performed on a single 420 nm nanocube displayed in Figure 4(d) clearly evidences the resonant light scattering due to the excitation of electric and magnetic multipoles. The photoluminescence spectrum of $CsPbBr_3$ is indicated by the green zone in Figure 4(d). A peak of the dark field spectrum can be observed in this spectral range. The resonant light scattering is assessed by observing a strong dependence of the scattering spectra on the size of the nanocubes. The photoluminescence spectra are recorded when exciting nanocubes with a 150 fs laser. Importantly, the spectra

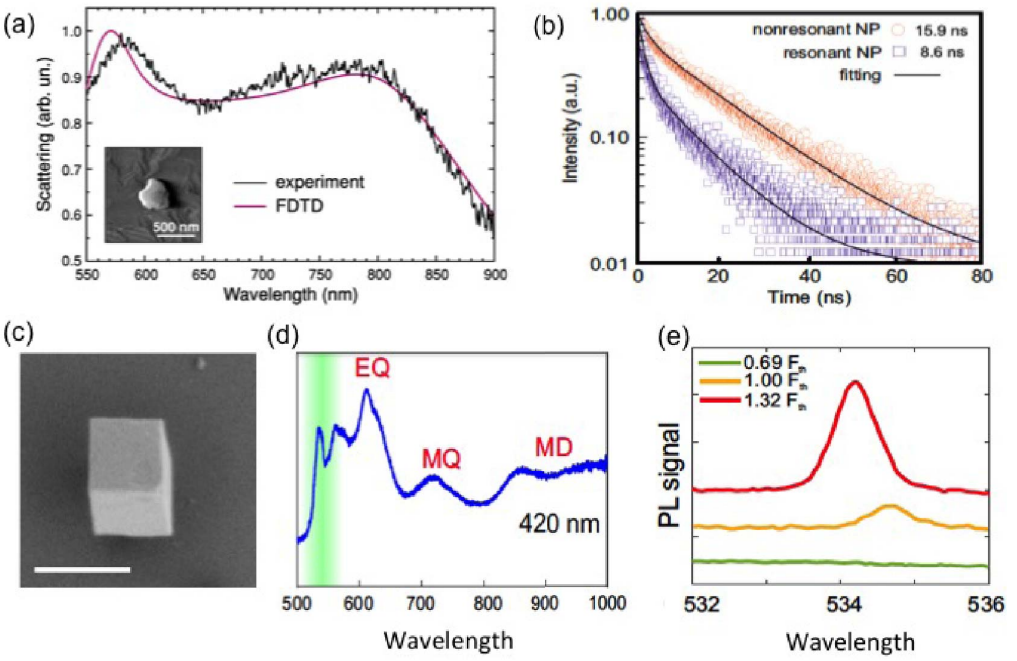

Figure 4. Mie resonances in excitonic materials: colored centers in nanodiamonds (top row) and perovskites (bottom row). (a) Unpolarized scattering spectrum of a single nanodiamond. Black line: experimental spectrum. Red line: numerical simulations implemented with FDTD (Finite Difference Time Domain) when considering a spherical nanodiamond with a diameter of 320 nm under the experimental conditions of the collection. Adapted with permission from [77]. (b) Time-resolved photoluminescence measurements for two sets of samples: NV centers in optically small (<100 nm) nanodiamonds (orange dots) and in large and optically resonant nanodiamonds (purple dots). Adapted with permission from [79]. (c) SEM images of $CsPbBr_3$ nanocubes placed on a sapphire substrate. Scale bar is 500 nm. (d) Dark-field spectra of the $CsPbBr_3$ nanocubes. The photoluminescence spectral range is indicated by the green zone. Pump intensity-dependent emission spectra for three different fluences compared with the lasing threshold: above (red), equal (orange) and below (green) the lasing threshold. (c–e) Adapted with permission from [83].

reveal a threshold-like appearance of a photoluminescence signal in the range $\lambda = (532; 538)$ nm, that corresponds to the red side of the emission line of the exciton (see Figure 4(e)).

5. Bound states in the continuum

Bound states in the continuum have attracted a lot of attention in photonics recently, and they originate from a coupling between the leaky modes in dielectric structures such as photonic crystals, metasurfaces, and isolated resonators [84]. These resonances provide an alternative mean to achieve very large Q factors for lasing [85] and also allow to tune a photonic system into the regime of the so-called *supercavity mode* [86]. A true bound state in the continuum (BIC) is a mathematical object with an infinite value of the Q factor and vanishing resonance width, and it can exist only in ideal loss-less infinite structures or for extreme values of parameters [87, 88]. In practice, BIC can be realized as a quasi-BIC mode, being directly associated with the supercavity

mode [86], when both the Q factor and resonance width become finite. However, the localization of light inspired by the BIC physics makes it possible to realize high-Q quasi-BIC modes in many optical structures such as cavities and coupled waveguides.

Importantly, there exists a direct link between quasi-BIC states and Fano resonances since these two phenomena are supported by the similar physics. More specifically, quasi-BIC resonance can be described explicitly by the classical Fano formula, and the observed peak positions and linewidths correspond exactly to the real and imaginary parts of the eigenmode frequencies. The Fano parameter becomes ill-defined at the BIC condition, which corresponds to a collapse of the Fano resonance. Importantly, every quasi-BIC modes can be linked with the Fano resonances, whereas the opposite is not always true: the Fano resonance may not converge to the BIC mode for any variation of the system parameters.

As an example, we consider all-dielectric metasurfaces with the in-plane symmetry breaking [89] that can support sharp high-Q resonances arising from a distortion of symmetry-protected BICs. We follow the recent paper [90], we consider a metasurface made of As_2S_3 and placed on a glass substrate consisting of a square lattice of meta-atoms with broken in-plane inversion symmetry, as illustrated in Figure 5(a). The meta-atom is constructed of a pair of rectangular bars which have lengths L and $L-\delta L$, respectively. The asymmetry of the unit cell is controlled by the difference in bar lengths, which is characterized by the asymmetry parameter $\alpha = \delta L/L$, see Figure 5(b).

Figure 5(c) demonstrates the dependence of the simulated transmission spectra on the wavelength of excitation and the asymmetry parameter α. The white dashed line illustrates the eigenmode dispersion. The eigenmode simulations show that the metasurface with a symmetric unit cell ($\alpha = 0$) supports a symmetry-protected BIC at 795 nm, which has infinite Q factor and is not manifested in the transmission spectrum. The BIC is unstable against perturbations that break the in-plane inversion symmetry, so for $\alpha > 0$ it transforms into a quasi-BIC with a finite Q factor [89]. The quasi-BIC is revealed in the transmission spectra as a sharp resonance with a Fano lineshape whose linewidth increases with the magnitude of asymmetry. The dependence of the radiative Q factor on α follows the inverse quadratic law for small values of the asymmetry parameter [89], as shown in Figure 5(d). Hence, the meta-atom asymmetry is necessary to obtain a sharp resonance whose position and width can be adjusted by the degree of asymmetry.

Thus, bound states in the continuum provide a new approach for engineering a resonant response of dielectric metasurfaces composed of meta-atoms with broken in-plane inversion symmetry. The similar approach can be applied to the case of nonlinear metasurfaces [91, 92] with broken-symmetry or nonlinear metasurfaces composed of arrays of chalcogenide nanoresonators designed for the nonlinear optical generation of higher harmonics.

6. Applications of Mie resonances: structural colors

Colors perceived by eyes result from the interaction between the incoming light and the three types of cone cells. A modification in the spectrum of the incoming light will result in a modification of the perceived color. When white light interacts with structured matter, its broad spectrum experiences a strong variation with peaks and dips which yield a color to the nanostructured matter. Colors resulting from the interaction between light and nano or microstructures are called structural colors. The terminology “structural” means that the color depends on the morphology of the structured matter. A modification of the morphology modifies the structural color. Structural colors can be found in a wide set of biological species, the most famous example being certainly the wings of the Morpho butterfly [93, 94]. Wings are structured at a sub-micrometer scale which provides photonic band gaps. In the case of the Morpho butterfly, the photonic band gap

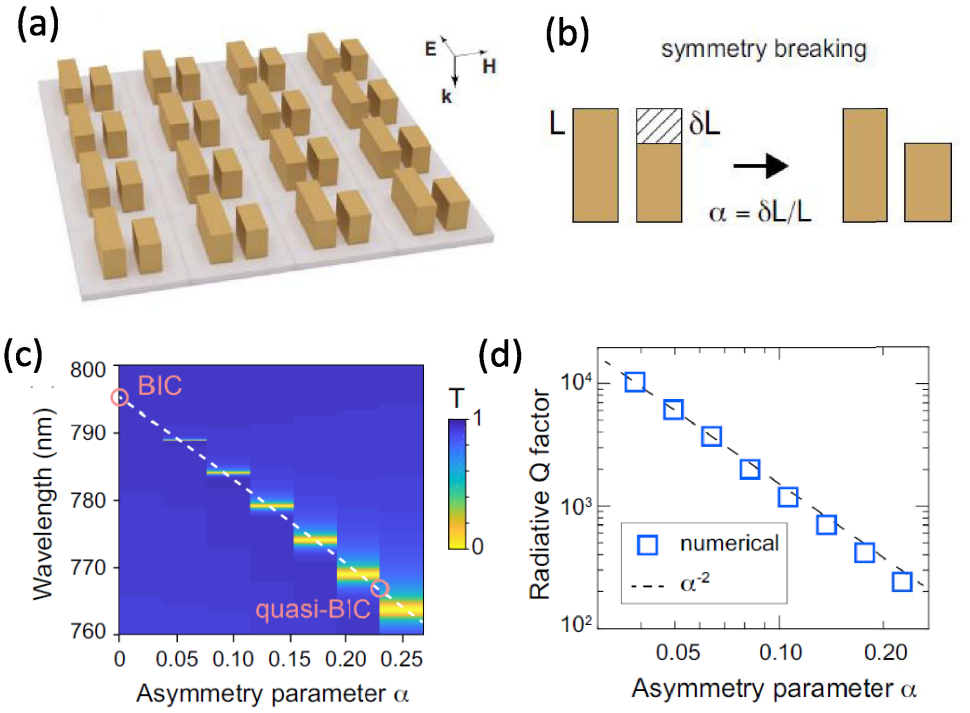

Figure 5. Metasurfaces with bound states in the continuum. (a) Design of a metasurface consisting of a square array of As_2S_3-bar pairs of different length placed on a glass substrate. The inset shows the orientation and polarization of the incident field. (b) Definition of the asymmetry parameter α. (c) Numerically simulated transmission spectra with respect to the excitation wavelength and the asymmetry parameter α. The white dashed line illustrates the quasi-BIC dispersion. (d) Dependence of the radiative Q factor on the parameter α. The dashed line shows an inverse quadratic fitting. Adapted with permission from [90].

is centered on the blue part of the spectrum. The blue part of the spectrum is therefore reflected which provides a vivid blue color to the wings.

Structural colors can also be found in plasmonics. When observing metallic particles of different sizes and shapes dispersed in a transparent substrate in dark field spectroscopy, a myriad of colors can be observed. It turns out that each particle yields its own color and behaves like a colored pixel. The pixel size stands under the diffraction limit and achieves the limit of resolution. This approach is very promising to create non fading colors with a high resolution. When assembling different scatterers on a surface, colored images can be finely designed which opens plenty of rooms to create images at high resolution [95]. Structural colors have benefited from intense developments to extend the gamut of colors, to decrease the cost of this technology and to extend its range of applications [96].

When observing silicon particles in dark-field spectroscopy, structural colors can also be observed (see Figure 1) [9, 10, 19, 97]. This result was expected since their resonant interaction with light strongly modulates the scattered spectrum. The coupling of light with electric and magnetic Mie resonant modes of high-index particles results in a perceived color that can be controlled through the shape and composition of the particles, and also through their mutual coupling. This result strengthens the field of resonant structural colors since cost effective and

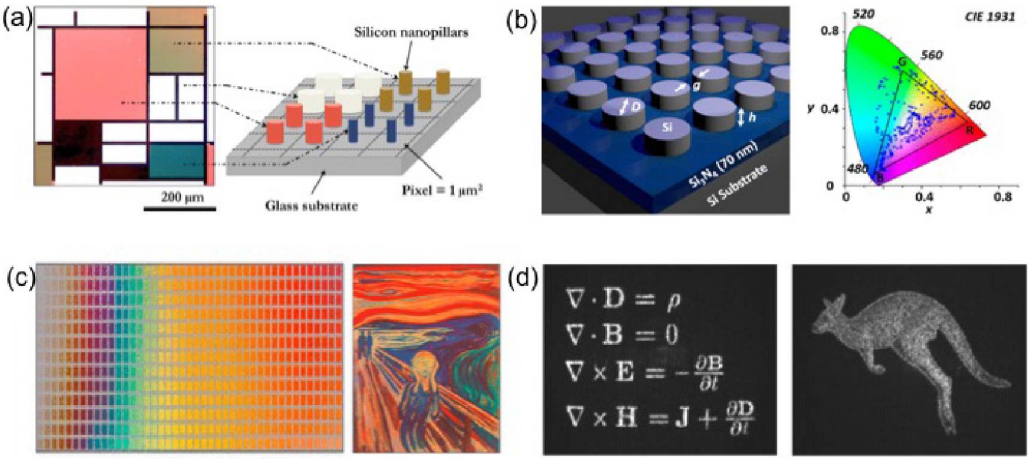

Figure 6. Silicon Mie-resonant metasurfaces for generating colors and holograms. (a) Mondrian's painting reproduced at a 1:1200 scale with silicon particles on a transparent substrate observed in dark-field imaging. Adapted with permission from [99]. (b) Extended gamut of colors obtained by coupling the nanostructured silicon layer with an unpatterned underlying high refractive index layer made of Si_3N_4. Adapted with permission from [100]. (c) Palette of colors obtained when varying the diameter of the silicon nanodisks and the period of the 2D array. Example of a painting reproduction. Here "The Scream" by the Norwegian painter Edvard Munch. Adapted with permission from [101]. (d) Experimental holographic images from two holograms at a 1600 nm wavelength. Adapted with permission from [106].

non toxic materials with high refractive index can be found. A strong interest has been brought to the case of silicon based nanostructures. One of the first examples of structural colours in silicon was presented in 2014 with periodical grooves patterned in silicon substrates [98]. When assembling silicon Mie resonators on a substrate and when controlling their size to tailor finely their spectral response, colored images can be obtained and painting can be reproduced. This was shown in 2016 in dark field spectroscopy with silicon particles of different diameters etched on a silicon film coated on a transparent substrate [99]. A palette of structural colors has been created when considering several arrays of similar Si nanodisks. In a second step, a Mondrian's painting was reproduced (Figure 6(a)). Mie resonant scatterers have been optimized to extend the gamut of colors, in particular through the control of their shape or through the coupling with an underlying layer [100] (see Figures 6(b,c)) or by adjusting the diameter of nanodisks and the period of the 2D array of nanodisks [101, 102]. This technique can also be employed to design spectral filters [102, 103]. Over the last two years, outstanding achievements have been reported in terms of designs and color rendering with different dielectric materials and fabrication methods [101, 104, 105]. The strong efforts devoted to the development of structural colors are motivated by numerous applications in anti-counterfeiting, spectral filtering, and color rendering of surfaces. The latest developments are focused on novel applications such as complex holograms [106, 107] (see Figure 6(d)).

7. Conclusion

The field of high-index dielectric metaphotonics has emerged recently as a new and rapidly developing direction of research in nanophotonics and metamaterials. The study of all-dielectric

resonant nanostructures is motivated by the rich physics of Mie resonances allowing to excite both electric and magnetic multipole modes in individual subwavelength particles. Metaphotonics has a broad range of applications, highlighting the importance of optically-induced magnetic response, and including structural coloring, optical sensing, spatial modulation of light, nonlinear and active media, as well as both integrated classical and quantum circuitry and topological photonics, underpinning a new generation of highly-efficient active metadevices. We anticipate further rapid development of these ideas into the field of *active metaphotonics* for creating new types of light sources, light-emitting metasurfaces, quantum signal processing, and efficient nanolasers.

References

[1] S. O'Brien, J. B. Pendry, "Photonic band-gap effects and magnetic activity in dielectric composites", *J. Phys.: Condens. Matter* **14** (2002), no. 15, p. 4035.
[2] J. A. Schuller, R. Zia, T. Taubner, M. L. Brongersma, "Dielectric metamaterials based on electric and magnetic resonances of silicon carbide particles", *Phys. Rev. Lett.* **99** (2007), article ID 107401.
[3] A. B. Evlyukhin, C. Reinhardt, A. Seidel, B. S. Luk'yanchuk, B. N. Chichkov, "Optical response features of si-nanoparticle arrays", *Phys. Rev. B* **82** (2010), article ID 045404.
[4] A. B. Evlyukhin, C. Reinhardt, B. N. Chichkov, "Multipole light scattering by nonspherical nanoparticles in the discrete dipole approximation", *Phys. Rev. B* **84** (2011), article ID 235429.
[5] A. García-Etxarri, R. Gómez-Medina, L. S. Froufe-Pérez, C. López, L. Chantada, F. Scheffold, J. Aizpurua, M. Nieto-Vesperinas, J. J. Sáenz, "Strong magnetic response of submicron silicon particles in the infrared", *Opt. Express* **19** (2011), no. 6, p. 4815-4826.
[6] A. Krasnok, A. Miroshnichenko, P. Belov, Y. Kivshar, "Huygens optical elements and Yagi–Uda nanoantennas based on dielectric nanoparticles", *JETP Lett.* **94** (2011), p. 593-598.
[7] B. Rolly, B. Stout, N. Bonod, "Boosting the directivity of optical antennas with magnetic and electric dipolar resonant particles", *Opt. Express* **20** (2012), no. 18, p. 20376-20386.
[8] A. E. Krasnok, A. E. Miroshnichenko, P. A. Belov, Y. S. Kivshar, "All-dielectric optical nanoantennas", *Opt. Express* **20** (2012), no. 18, p. 20599-20604.
[9] A. I. Kuznetsov, A. E. Miroshnichenko, Y. H. Fu, J. Zhang, B. Lukyanchuk, "Magnetic light", *Sci. Rep.* **2** (2012), p. 492.
[10] A. B. Evlyukhin, S. M. Novikov, U. Zywietz, R. L. Eriksen, C. Reinhardt, S. I. Bozhevolnyi, B. N. Chichkov, "Demonstration of magnetic dipole resonances of dielectric nanospheres in the visible region", *Nano Lett.* **12** (2012), no. 7, p. 3749-3755.
[11] A. I. Kuznetsov, A. E. Miroshnichenko, M. L. Brongersma, Y. S. Kivshar, B. Luk'yanchuk, "Optically resonant dielectric nanostructures", *Science* **354** (2016), no. 6314, article ID aag2472.
[12] S. Kruk, Y. Kivshar, "Functional meta-optics and nanophotonics governed by Mie resonances", *ACS Photon.* **4** (2017), p. 2638.
[13] G. Mie, "Beiträge zur optik trüber medien, speziell kolloidaler metallösungen", *Ann. Phys.* **330** (1908), no. 3, p. 377-445.
[14] H. Hulst, *Light scattering by small particles, Structure of matter series*, Wiley, 1957.
[15] A. Lagendijk, B. A. van Tiggelen, "Resonant multiple scattering of light", *Phys. Rep.* **270** (1996), no. 3, p. 143-215.
[16] A. B. Matsko, V. S. Ilchenko, "Optical resonators with whispering gallery modes i: basics", *IEEE J. Sel. Top. Quantum Electron.* **12** (2006), no. 3, p. 3.
[17] V. S. Ilchenko, A. B. Matsko, "Optical resonators with whispering-gallery modes-part ii: applications", *IEEE J. Sel. Top. Quantum Electron.* **12** (2006), no. 1, p. 15-32.
[18] A. Devilez, X. Zambrana-Puyalto, B. Stout, N. Bonod, "Mimicking localized surface plasmons with dielectric particles", *Phys. Rev. B* **92** (2015), no. 24, article ID 241412.
[19] U. Zywietz, A. B. Evlyukhin, C. Reinhardt, B. N. Chichkov, "Laser printing of silicon nanoparticles with resonant optical electric and magnetic responses", *Nat. Commun.* **5** (2014), p. 3402.
[20] F. B. Arango, A. F. Koenderink, "Polarizability tensor retrieval for magnetic and plasmonic antenna design", *New J. Phys.* **15** (2013), no. 7, article ID 073023.
[21] J. Proust, N. Bonod, J. Grand, B. Gallas, "Optical monitoring of the magnetoelectric coupling in individual plasmonic scatterers", *ACS Photon.* **3** (2016), no. 9, p. 1581-1588.
[22] M. Dubois, L. Leroi, Z. Raolison, R. Abdeddaim, T. Antonakakis, J. de Rosny, A. Vignaud, P. Sabouroux, E. Georget, B. Larrat *et al.*, "Kerker effect in ultrahigh-field magnetic resonance imaging", *Phys. Rev. X* **8** (2018), no. 3, article ID 031083.

[23] P. Nordlander, C. Oubre, E. Prodan, K. Li, M. Stockman, "Plasmon hybridizaton in nanoparticle dimers", *Nano Lett.* **4** (2004), no. 5, p. 899-903.
[24] M. Kerker, D.-S. Wang, C. L. Giles, "Electromagnetic scattering by magnetic spheres", *J. Opt. Soc. Am.* **73** (1983), no. 6, p. 765-767.
[25] R. Gomez-Medina, B. Garcia-Camara, I. Suarez-Lacalle, F. Gonzalez, F. Moreno, M. Nieto-Vesperinas, J. J. Saenz, "Electric and magnetic dipolar response of germanium nanospheres: interference effects, scattering anisotropy, and optical forces", *J. Nanophoton.* **5** (2011), article ID 053512.
[26] M. Nieto-Vesperinas, R. Gomez-Medina, J. J. Saenz, "Angle-suppressed scattering and optical forces on submicrometer dielectric particles", *J. Opt. Soc. Am. A* **28** (2011), no. 1, p. 54-60.
[27] S. Person, M. Jain, Z. Lapin, J. J. Saenz, G. Wicks, L. Novotny, "Demonstration of zero optical backscattering from single nanoparticles", *Nano Lett.* **13** (2013), no. 4, p. 1806-1809.
[28] H. Shamkhi, K. Baryshnikova, A. Sayanskiy, P. Kapitanova, P. Terekhov, P. Belov, A. Karabchevsky, A. Evlyukhin, Y. Kivshar, A. Shalin, "Transverse scattering and generalized Kerker effects in all-dielectric mie-resonant metaoptics", *Phys. Rev. Lett.* **122** (2019), article ID 193905.
[29] R. Paniagua-Domínguez, F. López-Tejeira, R. Marqués, J. A. Sánchez-Gil, "Metallo-dielectric core-shell nanospheres as building blocks for optical three-dimensional isotropic negative-index metamaterials", *New J. Phys.* **13** (2011), no. 12, article ID 123017.
[30] J. Geffrin, B. García-Cámara, R. Gómez-Medina, P. Albella, L. Froufe-Pérez, C. Eyraud, A. Litman, R. Vaillon, F. González, M. Nieto-Vesperinas *et al.*, "Magnetic and electric coherence in forward-and back-scattered electromagnetic waves by a single dielectric subwavelength sphere", *Nat. Commun.* **3** (2012), p. 1171.
[31] Y. H. Fu, A. I. Kuznetsov, A. E. Miroshnichenko, Y. F. Yu, B. Lukyanchuk, "Directional visible light scattering by silicon nanoparticles", *Nat. Commun.* **4** (2013), p. 1527.
[32] I. Staude, A. E. Miroshnichenko, M. Decker, N. T. Fofang, S. Liu, E. Gonzales, J. Dominguez, T. S. Luk, D. N. Neshev, I. Brener *et al.*, "Tailoring directional scattering through magnetic and electric resonances in subwavelength silicon nanodisks", *ACS Nano* **7** (2013), no. 9, p. 7824-7832.
[33] B. S. Luk'yanchuk, N. V. Voshchinnikov, R. Paniagua-Domínguez, A. I. Kuznetsov, "Optimum forward light scattering by spherical and spheroidal dielectric nanoparticles with high refractive index", *ACS Photon.* **2** (2015), no. 7, p. 993-999.
[34] P. Moitra, B. A. Slovick, W. Li, I. I. Kravchencko, D. P. Briggs, S. Krishnamurthy, J. Valentine, "Large-scale all-dielectric metamaterial perfect reflectors", *ACS Photon.* **2** (2015), no. 6, p. 692-698.
[35] W. Liu, Y. Kivshar, "Generalized kerker effects in nanophotonics and meta-optics", *Opt. Express* **26** (2018), p. 13085-13105.
[36] H. K. Shamkhi, A. Sayanskiy, A. C. Valero, A. S. Kupriianov, P. Kapitanova, Y. S. Kivshar, A. S. Shalin, V. R. Tuz, "Transparency and perfect absorption of all-dielectric resonant metasurfaces governed by the transverse kerker effect", *Phys. Rev. Mater.* **3** (2019), no. 8, article ID 085201.
[37] M. Rybin, D. Filonov, P. Belov, Y. Kivshar, M. Limonov, "Switching from visibility to invisibility via fano resonances: Theory and experiment", *Sci. Rep.* **5** (2015), p. 8774.
[38] Q. Zhao, J. Zhou, F. Zhang, D. Lippens, "Mie resonance-based dielectric metamaterials", *Mater. Today* **12** (2009), p. 60-69.
[39] J. Valentine, J. Li, T. Zentgraf, G. Bartal, X. Zhang, "An optical cloak made of dielectrics", *Nat. Mater.* **8** (2009), p. 568-571.
[40] M. M. Farhat, S. Muhlig, C. Rockstuhl, F. Lederer, "Scattering cancellation of the magnetic dipole field from macroscopic spheres", *Opt. Express* **20** (2012), p. 13896-13906.
[41] L. Novotny, N. van Hulst, "Antennas for light", *Nat. Photon.* **5** (2011), no. 2, p. 83-90.
[42] E. Dulkeith, A. Morteani, T. Niedereichholz, T. Klar, J. Feldmann, S. Levi, F. Van Veggel, D. Reinhoudt, M. Möller, D. Gittins, "Fluorescence quenching of dye molecules near gold nanoparticles: radiative and nonradiative effects", *Phys. Rev. Lett.* **89** (2002), no. 20, article ID 203002.
[43] P. Mühlschlegel, H. Eisler, O. Martin, B. Hecht, D. Pohl, "Resonant optical antennas", *Science* **308** (2005), no. 5728, p. 1607-1609.
[44] P. Anger, P. Bharadwaj, L. Novotny, "Enhancement and quenching of single-molecule fluorescence", *Phys. Rev. Lett.* **96** (2006), article ID 113002.
[45] P. Bharadwaj, L. Novotny, "Spectral dependence of single molecule fluorescence enhancement", *Opt. Express* **15** (2007), no. 21, p. 14266-14274.
[46] M. Ringler, A. Schwemer, M. Wunderlich, A. Nichtl, K. Kürzinger, T. Klar, J. Feldmann, "Shaping emission spectra of fluorescent molecules with single plasmonic nanoresonators", *Phys. Rev. Lett.* **100** (2008), no. 20, article ID 203002.
[47] J. Li, A. Salandrino, N. Engheta, "Shaping light beams in the nanometer scale: A Yagi–Uda nanoantenna in the optical domain", *Phys. Rev. B* **76** (2007), article ID 245403.
[48] A. G. Curto, G. Volpe, T. H. Taminiau, M. P. Kreuzer, R. Quidant, N. F. van Hulst, "Unidirectional emission of a quantum dot coupled to a nanoantenna", *Science* **329** (2010), no. 5994, p. 930-933.

[49] H. Aouani, O. Mahboub, N. Bonod, E. Devaux, E. Popov, H. Rigneault, T. W. Ebbesen, J. Wenger, "Bright unidirectional fluorescence emission of molecules in a nanoaperture with plasmonic corrugations", *Nano Lett.* **11** (2011), no. 2, p. 637-644.
[50] M. P. Busson, B. Rolly, B. Stout, N. Bonod, S. Bidault, "Accelerated single photon emission from dye molecule-driven nanoantennas assembled on DNA", *Nat. Commun.* **3** (2012), p. 962.
[51] G. Acuna, F. Möller, P. Holzmeister, S. Beater, B. Lalkens, P. Tinnefeld, "Fluorescence enhancement at docking sites of DNA-directed self-assembled nanoantennas", *Science* **338** (2012), no. 6106, p. 506-510.
[52] T. B. Hoang, G. M. Akselrod, M. H. Mikkelsen, "Ultrafast room-temperature single photon emission from quantum dots coupled to plasmonic nanocavities", *Nano Lett.* **16** (2015), no. 1, p. 270-275.
[53] J. J. Baumberg, J. Aizpurua, M. H. Mikkelsen, D. R. Smith, "Extreme nanophotonics from ultrathin metallic gaps", *Nat. Mater.* **18** (2019), p. 668-678.
[54] D. Gérard, A. Devilez, H. Aouani, B. Stout, N. Bonod, J. Wenger, E. Popov, H. Rigneault, "Efficient excitation and collection of single-molecule fluorescence close to a dielectric microsphere", *J. Opt. Soc. Am. B* **26** (2009), no. 7, p. 1473-1478.
[55] A. Devilez, B. Stout, N. Bonod, "Compact metallo-dielectric optical antenna for ultra directional and enhanced radiative emission", *ACS Nano* **4** (2010), no. 6, p. 3390-3396.
[56] J. Ho, Y. H. Fu, Z. Dong, R. Paniagua-Dominguez, E. H. Koay, Y. F. Yu, V. Valuckas, A. I. Kuznetsov, J. K. Yang, "Highly directive hybrid metal–dielectric Yagi–Uda nanoantennas", *ACS Nano* **12** (2018), no. 8, p. 8616-8624.
[57] S. Bidault, M. Mivelle, N. Bonod, "Dielectric nanoantennas to manipulate solid-state light emission", *J. Appl. Phys.* **126** (2019), no. 9, article ID 094104.
[58] D. G. Baranov, R. S. Savelev, S. V. Li, A. E. Krasnok, A. Alù, "Modifying magnetic dipole spontaneous emission with nanophotonic structures", *Laser Photon. Rev.* **11** (2017), no. 3, article ID 1600268.
[59] S. Karaveli, R. Zia, "Strong enhancement of magnetic dipole emission in a multilevel electronic system", *Opt. Lett.* **35** (2010), no. 20, p. 3318-3320.
[60] S. Karaveli, R. Zia, "Spectral tuning by selective enhancement of electric and magnetic dipole emission", *Phys. Rev. Lett.* **106** (2011), article ID 193004.
[61] C. M. Dodson, R. Zia, "Magnetic dipole and electric quadrupole transitions in the trivalent lanthanide series: Calculated emission rates and oscillator strengths", *Phys. Rev. B* **86** (2012), article ID 125102.
[62] B. Rolly, B. Bebey, S. Bidault, B. Stout, N. Bonod, "Promoting magnetic dipolar transition in trivalent lanthanide ions with lossless mie resonances", *Phys. Rev. B* **85** (2012), article ID 245432.
[63] M. K. Schmidt, R. Esteban, J. J. Sáenz, I. Suárez-Lacalle, S. Mackowski, J. Aizpurua, "Dielectric antennas - a suitable platform for controlling magnetic dipolar emission", *Opt. Express* **20** (2012), no. 13, p. 13636-13650.
[64] M. Sanz-Paz, C. Ernandes, J. U. Esparza, G. W. Burr, N. F. van Hulst, A. Maitre, L. Aigouy, T. Gacoin, N. Bonod, M. F. Garcia-Parajo *et al.*, "Enhancing magnetic light emission with all-dielectric optical nanoantennas", *Nano Lett.* **18** (2018), no. 6, p. 3481-3487.
[65] A. Vaskin, S. Mashhadi, M. Steinert, K. E. Chong, D. Keene, S. Nanz, A. Abass, E. Rusak, D.-Y. Choi, I. Fernandez-Corbaton, T. Pertsch, C. Rockstuhl, M. A. Noginov, Y. S. Kivshar, D. N. Neshev, N. Noginova, I. Staude, "Manipulation of magnetic dipole emission from eu3+ with mie-resonant dielectric metasurfaces", *Nano Lett.* **19** (2019), no. 2, p. 1015-1022.
[66] M. Sigalas, D. Fattal, R. Williams, S. Wang, R. Beausoleil, "Electric field enhancement between two si microdisks", *Opt. Express* **15** (2007), no. 22, p. 14711-14716.
[67] J. Cambiasso, G. Grinblat, Y. Li, A. Rakovich, E. Cortés, S. A. Maier, "Bridging the gap between dielectric nanophotonics and the visible regime with effectively lossless gallium phosphide antennas", *Nano Lett.* **17** (2017), no. 2, p. 1219-1225.
[68] R. Regmi, J. Berthelot, P. M. Winkler, M. Mivelle, J. Proust, F. Bedu, I. Ozerov, T. Begou, J. Lumeau, H. Rigneault *et al.*, "All-dielectric silicon nanogap antennas to enhance the fluorescence of single molecules", *Nano Lett.* **16** (2016), no. 8, p. 5143-5151.
[69] A. Kinkhabwala, Z. Yu, S. Fan, Y. Avlasevich, K. Mullen, W. E. Moerner, "Large single-molecule fluorescence enhancements produced by a bowtie nanoantenna", *Nat. Photon.* **3** (2009), no. 11, p. 654-657.
[70] D. Punj, M. Mivelle, S. B. Moparthi, T. S. Van Zanten, H. Rigneault, N. F. Van Hulst, M. F. García-Parajó, J. Wenger, "A plasmonic antenna-in-box platform for enhanced single-molecule analysis at micromolar concentrations", *Nat. Nanotechnol.* **8** (2013), no. 7, p. 512.
[71] P. Albella, M. A. Poyli, M. K. Schmidt, S. A. Maier, F. Moreno, J. J. Sáenz, J. Aizpurua, "Low-loss electric and magnetic field-enhanced spectroscopy with subwavelength silicon dimers", *J. Phys. Chem. C* **117** (2013), no. 26, p. 13573-13584.
[72] M. Caldarola, P. Albella, E. Cortés, M. Rahmani, T. Roschuk, G. Grinblat, R. F. Oulton, A. V. Bragas, S. A. Maier, "Non-plasmonic nanoantennas for surface enhanced spectroscopies with ultra-low heat conversion", *Nat. Commun.* **6** (2015), p. 7915.

[73] X. Zambrana-Puyalto, N. Bonod, "Purcell factor of spherical mie resonators", *Phys. Rev. B* **91** (2015), no. 19, article ID 195422.
[74] V. Rutckaia, F. Heyroth, A. Novikov, M. Shaleev, M. Petrov, J. Schilling, "Quantum dot emission driven by mie resonances in silicon nanostructures", *Nano Lett.* **17** (2017), no. 11, p. 6886-6892.
[75] K. Frizyuk, M. Hasan, A. Krasnok, A. Alú, M. Petrov, "Enhancement of Raman scattering in dielectric nanostructures with electric and magnetic mie resonances", *Phys. Rev. B* **97** (2018), no. 8, article ID 085414.
[76] D. G. Baranov, R. Verre, P. Karpinski, M. Kall, "Anapole-enhanced intrinsic Raman scattering from silicon nanodisks", *ACS Photon.* **5** (2018), no. 7, p. 2730-2736.
[77] D. A. Shilkin, M. R. Shcherbakov, E. V. Lyubin, K. G. Katamadze, O. S. Kudryavtsev, V. S. Sedov, I. I. Vlasov, A. A. Fedyanin, "Optical magnetism and fundamental modes of nanodiamonds", *ACS Photon.* **4** (2017), no. 5, p. 1153-1158.
[78] R. Savelev, A. Zalogina, S. Kudryashov, A. Ivanova, A. Levchenko, S. Makarov, D. Zuev, I. Shadrivov, "Control of spontaneous emission rate in luminescent resonant diamond particles", *J. Phys.: Conf. Ser.* **961** (2018), article ID 012007.
[79] A. Zalogina, R. Savelev, E. Ushakova, G. Zograf, F. Komissarenko, V. Milichko, S. Makarov, D. Zuev, I. Shadrivov, "Purcell effect in active diamond nanoantennas", *Nanoscale* **10** (2018), no. 18, p. 8721-8727.
[80] S. Makarov, A. Furasova, E. Tiguntseva, A. Hemmetter, A. Berestennikov, A. Pushkarev, A. Zakhidov, Y. Kivshar, "Halide-perovskite resonant nanophotonics", *Adv. Opt. Mater.* **7** (2019), no. 1, article ID 1800784.
[81] A. S. Berestennikov, P. M. Voroshilov, S. V. Makarov, Y. S. Kivshar, "Active meta-optics and nanophotonics with halide perovskites", *Appl. Phys. Rev.* **6** (2019), no. 3, article ID 031307.
[82] E. Y. Tiguntseva, G. P. Zograf, F. E. Komissarenko, D. A. Zuev, A. A. Zakhidov, S. V. Makarov, Y. S. Kivshar, "Light-emitting halide perovskite nanoantennas", *Nano Lett.* **18** (2018), no. 2, p. 1185-1190.
[83] E. Tiguntseva, K. Koshelev, A. Furasova, P. Tonkaev, V. Mikhailovskii, E. V. Ushakova, D. G. Baranov, T. Shegai, A. A. Zakhidov, Y. Kivshar *et al.*, "Room-temperature lasing from mie-resonant non-plasmonic nanoparticles", *ACS Nano* **14** (2020), no. 7, p. 8149-8156.
[84] C. Hsu, B. Zhen, A. Stone, J. Joannopoulos, M. Soljacić, "Bound states in the continuum", *Nat. Rev. Mater.* **1** (2016), article ID 16048.
[85] A. Kodigala, T. Lepetit, Q. Gu, B. Bahari, Y. Fainman, B. Kanté, "Lasing action from photonic bound states in continuum", *Nature* **541** (2017), p. 196-199.
[86] M. Rybin, Y. Kivshar, "Supercavity lasing", *Nature* **541** (2017), p. 165-166.
[87] C. Hsu, B. Zhen, J. Lee, S. Chua, S. Johnson, J. Joannopoulos, "Observation of trapped light within the radiation continuum", *Nature* **499** (2013), p. 188-191.
[88] F. Monticone, A. Alu, "Embedded photonic eigenvalues in 3d nanostructures", *Phys. Rev. Lett.* **112** (2014), article ID 213903.
[89] K. Koshelev, S. Lepeshov, M. Liu, A. Bogdanov, Y. Kivshar, "Asymmetric metasurfaces with high-Q resonances governed by bound states in the continuum", *Phys. Rev. Lett.* **121** (2018), no. 19, article ID 193903.
[90] E. Mikheeva, K. Koshelev, D.-Y. Choi, S. Kruk, J. Lumeau, R. Abdeddaim, I. Voznyuk, S. Enoch, Y. Kivshar, "Photosensitive chalcogenide metasurfaces supporting bound states in the continuum", *Opt. Express* **27** (2019), p. 33847-33853.
[91] L. Wang, S. Kruk, K. Koshelev, I. Kravchenko, B. Luther-Davies, Y. Kivshar, "Nonlinear wavefront control with all-dielectric metasurfaces", *Nano Lett.* **18** (2018), no. 6, p. 3978.
[92] K. Koshelev, Y. Tang, K. Li, D.-Y. Choi, G. Li, Y. Kivshar, "Nonlinear metasurfaces governed by bound states in the continuum", *ACS Photon.* **6** (2019), no. 7, p. 1639.
[93] B. Gralak, G. Tayeb, S. Enoch, "Morpho butterflies wings color modeled with lamellar grating theory", *Opt. Express* **9** (2001), no. 11, p. 567-578.
[94] P. Vukusic, J. R. Sambles, "Photonic structures in biology", *Nature* **424** (2003), no. 6950, p. 852.
[95] K. Kumar, H. Duan, R. S. Hegde, S. C. Koh, J. N. Wei, J. K. Yang, "Printing colour at the optical diffraction limit", *Nat. Nanotechnol.* **7** (2012), no. 9, p. 557.
[96] A. Kristensen, J. K. Yang, S. I. Bozhevolnyi, S. Link, P. Nordlander, N. J. Halas, N. A. Mortensen, "Plasmonic colour generation", *Nat. Rev. Mater.* **2** (2017), no. 1, article ID 16088.
[97] M. Abbarchi, M. Naffouti, B. Vial, A. Benkouider, L. Lermusiaux, L. Favre, A. Ronda, S. Bidault, I. Berbezier, N. Bonod, "Wafer scale formation of monocrystalline silicon-based mie resonators via silicon-on-insulator dewetting", *ACS Nano* **8** (2014), no. 11, p. 11181-11190.
[98] E. Højlund-Nielsen, J. Weirich, J. Nørregaard, J. Garnaes, N. A. Mortensen, A. Kristensen, "Angle-independent structural colors of silicon", *J. Nanophoton.* **8** (2014), no. 1, article ID 083988.
[99] J. Proust, F. Bedu, B. Gallas, I. Ozerov, N. Bonod, "All-dielectric colored metasurfaces with silicon mie resonators", *ACS Nano* **10** (2016), no. 8, p. 7761-7767.
[100] Z. Dong, J. Ho, Y. F. Yu, Y. H. Fu, R. Paniagua-Dominguez, S. Wang, A. I. Kuznetsov, J. K. Yang, "Printing beyond srgb color gamut by mimicking silicon nanostructures in free-space", *Nano Lett.* **17** (2017), no. 12, p. 7620-7628.

[101] V. Flauraud, M. Reyes, R. Paniagua-Dominguez, A. I. Kuznetsov, J. Brugger, "Silicon nanostructures for bright field full color prints", *ACS Photon.* **4** (2017), no. 8, p. 1913-1919.
[102] V. Vashistha, G. Vaidya, R. S. Hegde, A. E. Serebryannikov, N. Bonod, M. Krawczyk, "All-dielectric metasurfaces based on cross-shaped resonators for color pixels with extended gamut", *ACS Photon.* **4** (2017), no. 5, p. 1076-1082.
[103] T. Wood, M. Naffouti, J. Berthelot, T. David, J.-B. Claude, L. Métayer, A. Delobbe, L. Favre, A. Ronda, I. Berbezier *et al.*, "All-dielectric color filters using sige-based mie resonator arrays", *ACS Photon.* **4** (2017), no. 4, p. 873-883.
[104] X. Zhu, W. Yan, U. Levy, N. A. Mortensen, A. Kristensen, "Resonant laser printing of structural colors on high-index dielectric metasurfaces", *Sci. Adv.* **3** (2017), no. 5, article ID e1602487.
[105] S. Sun, Z. Zhou, C. Zhang, Y. Gao, Z. Duan, S. Xiao, Q. Song, "All-dielectric full-color printing with tio2 metasurfaces", *ACS Nano* **11** (2017), no. 5, p. 4445-4452.
[106] L. Wang, S. Kruk, H. Tang, T. Li, I. Kravchenko, D. N. Neshev, Y. S. Kivshar, "Grayscale transparent metasurface holograms", *Optica* **3** (2016), no. 12, p. 1504-1505.
[107] H. Ren, G. Briere, X. Fang, P. Ni, R. Sawant, S. Héron, S. Chenot, S. Vézian, B. Damilano, V. Brändli *et al.*, "Metasurface orbital angular momentum holography", *Nat. Commun.* **10** (2019), no. 1, p. 2986.